IEEE Transactions on Nuclear Science, Vol.NS-21, June 1974

A Tutorial on ART
(Algebraic Reconstruction Techniques)

Richard Gordon
Mathematical Research Branch
National Institute of Arthritis, Metabolism and Digestive Diseases
Bethesda, Maryland 20014, USA

I. Introduction

Algebraic Reconstruction Techniques (ART) were introduced by Gordon, Bender & Herman (1970) for solving the problem of three dimensional reconstruction from projections in electron microscopy and radiology. This is a deconvolution problem of a particular type: an estimate of a function in a higher dimensional space is deconvolved from its experimentally measured projections to a lower dimensional space. For instance, an x-ray photograph represents the projection of the three-dimensional distribution of x-ray densities within the body onto a two-dimensional plane. A finite number of such photographs taken at different angles allows us to reconstruct an estimate of the original 3-D densities. ('Density refers to optical density.)

The ART algorithms for solving this problem have a simple intuitive basis. Each projected density is thrown back across the higher dimensional region from whence it came, with repeated corrections to bring each projection of the estimate into agreement with the corresponding measured projection.

In order to discuss the ART algorithms, one must first carefully consider the representation of space in digital computers (Sections II and III). Subsequent sections will survey the original ART algorithm (Section IV), convergence criteria (Section V), variations on the ART algorithm (Section VI), reliability of reconstructions (Section VII) and computing efficiency (Section VIII).

All symbols used are summarized in Table 1.

II. The Representation of Space

In digital computers it is necessary to represent continuous space in a discrete fashion. Many truncated basis sets have been used to represent the higher dimensional space in reconstruction problems (Gordon & Herman, 1974). However, the ART algorithms are formulated in terms of a particular kind of basis set: one which divides the reconstruction space into a finite number of nonoverlapping elements or subregions. The unknown density distribution is approximated by the values assigned to each element by the reconstruction algorithm.

Let us assume that the unknown density function is identically zero outside a finite region $\mathcal{R}$. Let the reconstruction space $\mathcal{R}$ be divided into n nonoverlapping elements (Figure 1). Ideally we might want this division to be as fine as possible. The minimum fineness of the division of $\mathcal{R}$ is linked to our computer representation of the projections to the lower dimensional space.

Let us assume that each projection, which will be of finite extent, is also divided into nonoverlapping elements. The maximum size of the projection elements should be dictated by the presumed spatial resolution in the projection. (This resolution is determined by the physics of the radiation used.) It is common practice to use a spacing between elements which is half of the presumed resolution. (Finer division may be warranted if one is attempting to achieve superresolution by deconvoluting the spread function.)

Let $\mathcal{P}_j$, j=1,...,m, represent all the projection elements of the available projections taken together. For each projected element $\mathcal{P}_j$ there is a corresponding subregion $\mathcal{S}_j$ in $\mathcal{R}$ of which $\mathcal{P}_j$ is the projection. The exact shape of $\mathcal{S}_j$ depends on the paths of the radiation through $\mathcal{R}$. $\mathcal{S}_j$ will be referred to as the passage for radiation falling on $\mathcal{P}_j$.

Let $\vec{r}$ represent a point in $\mathcal{R}$ and $f(\vec{r})$ our unknown density function. Then

$$\int_{\mathcal{S}_j} f(\vec{r})\, d\vec{r} \approx p_j \qquad j=1,\ldots,m \tag{1}$$

where p_j is the experimental measurement of the j^{th} projection element of $f(\vec{r})$. The approximation sign ($\approx$)

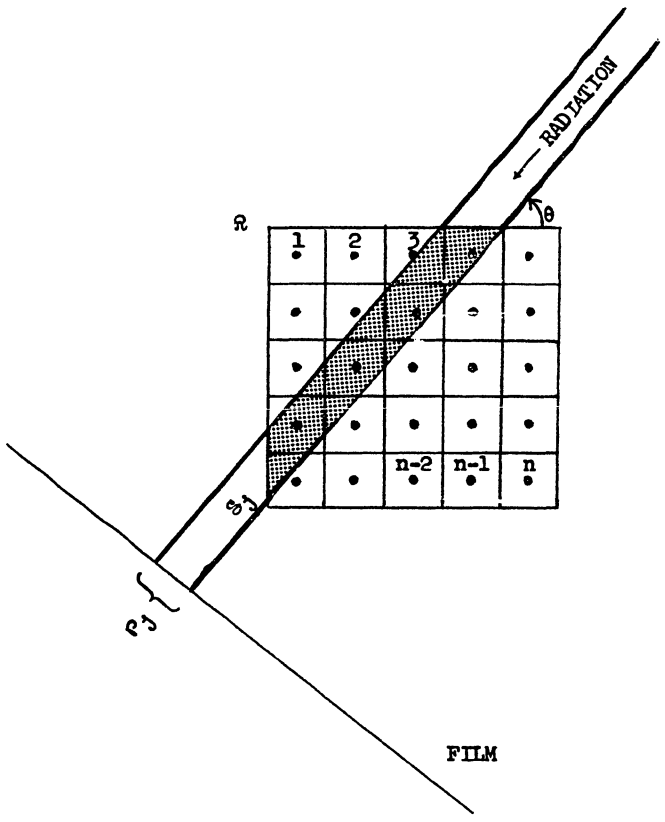

Figure 1. Illustration of the geometry of reconstruction from projections. The large square is a two-dimensional reconstruction space $\mathcal{R}$. It is divided into n small squares or reconstruction elements $\mathcal{R}_i$, i=1,...,m, each of which is to be assigned a value f_i. The centroids $\vec{r}_i$ are indicated by dots. Radiation impinges on the film or detector at projection element ρ_j giving the measurement p_j. This radiation has traversed the object through the passage $\mathcal{S}_j$, which is shaded. In this particular case the radiation travels in a parallel ray at angle θ and the ray width is chosen so that one centroid is encountered per row of elements $\mathcal{R}_i$ by $\mathcal{S}_j$, except for the last row. If we were to disregard this edge effect, then c_j would be identically 1. The shaded parts of the small squares represent $\mathcal{S}_j \cap \mathcal{R}_i$. Their areas are the w_{ij}. For a given square $\mathcal{R}_i$, u_{ij} = 1 if its centroid $\vec{r}_i$ is in the shaded region $\mathcal{S}_j$, = 0 if not.

indicates that the measurement process is not perfect. Equations 1 are the fundamental equations from which all reconstruction methods for determining $f(\vec{r})$ begin.

The passage $\mathcal{S}_j$ through $\mathcal{R}$ has no necessary geometric relationship to the elements of $\mathcal{R}$. Let $\mathcal{R}_i$ be the i^{th} element of $\mathcal{R}$. Then we may define the region $\mathcal{S}_j \cap \mathcal{R}_i$ as the intersection of passage $\mathcal{S}_j$ with the reconstruction element $\mathcal{R}_i$. This allows us to rewrite Equation 1 as

$$p_j \approx \sum_{i=1}^{n} \int_{\mathcal{S}_j \cap \mathcal{R}_i} f(\vec{r})\, d\vec{r} \qquad j=1,\ldots,m \tag{2}$$

Our goal is to obtain an approximation for the unknown function $f(\vec{r})$ by assigning an estimate f_i of its value to each region $\mathcal{R}_i$. The best estimate would result when f_i is the average value of $f(\vec{r})$ over the subregion $\mathcal{R}_i$:

$$f_i = \frac{\int_{\mathcal{R}_i} f(\vec{r})\, d\vec{r}}{\int_{\mathcal{R}_i} d\vec{r}} \qquad i=1,\ldots,n \tag{3}$$

This ideal outcome cannot be attained due to limitations on the amount and quality of data as well as the reconstruction algorithms themselves.

Since we are ignorant of how the function $f(\vec{r})$ varies within the element $\mathcal{R}_i$, we do not know its value in $\mathcal{S}_j \cap \mathcal{R}_i$. However, we may make the assumption that if f_i is the average value of $f(\vec{r})$ over $\mathcal{R}_i$ then the integral of $f(\vec{r})$ over $\mathcal{S}_j \cap \mathcal{R}_i$ may be estimated by the geometric fraction

$$w_{ij} = \frac{\int_{S_j \cap R_i} d\vec{r}}{\int_{R_i} d\vec{r}} \qquad i=1,\ldots,n \tag{4}$$

multiplied by f_i:

$$\int_{S_j \cap R_i} f(\vec{r})\, d\vec{r} \approx w_{ij}\, f_i \qquad i=1,\ldots,n;\ j=1,\ldots,m \tag{5}$$

By this further approximation, Equations 2 become a set of simultaneous linear equations in the unknowns f_i:

$$p_j \approx \sum_{i=1}^{n} w_{ij}\, f_i \qquad j=1,\ldots,m \tag{6}$$

Although these look like an ordinary set of linear equations, they are distinguished by a number of features:

1) The matrix $\{w_{ij}\}$ is quite sparse, since from the geometry of projections $S_j \cap R_i = \emptyset$, (the null set), for most pairs (i,j). (That is, only a relatively few of the w_{ij} are nonzero. Each passage S_j encounters only a relatively few of the R_i.)
2) The size of the matrix $\{w_{ij}\}$ can be enormous. In typical applications n starts at 2500 and with little ambition n can easily reach 10^6. In some cases $n = 10^9$. The number of projection elements m ranges from 500 to 10^5 and 10^7 in corresponding cases. Thus the matrix size nm ranges from 750,000 to 10^{11} or 10^{16}.
3) The equations are ordinarily highly underdetermined, i.e., $m << n$.
4) The rank of the matrix $\{w_{ij}\}$ is unknown.
5) The matrix $\{w_{ij}\}$ is nonnegative since $w_{ij} \geq 0$.
6) The data values p_j are ordinarily nonnegative.
7) The unknown function $f(\vec{r})$ is ordinarily assumed to be nonnegative, so that one desires a solution for which $f_i \geq 0$.
8) The errors in the data may cause the equations to be inconsistent.
9) Statistical effects of noise in the data should be analyzed, if possible.
10) The approximations by which we arrive at Equations 6 introduce systematic errors which have yet to be analyzed.

III. Efficient Representation of Space

Because of the enormity of the matrix $\{w_{ij}\}$ we must go to great lengths to reduce the size of the reconstruction problem.

In the interest of retaining detail in our estimate of the unknown density $f(\vec{r})$, the division of R should be made as fine as possible. On the other hand, the size of the matrix $\{w_{ij}\}$ directly depends on the number of elements into which R is divided, so that the division of R should be as coarse as possible. The size of the projection elements, however, limits the coarseness of the division of R. How this limit comes in may best be seen by considering a further approximation.

Let $\vec{r}_i$ be the centroid of the element R_i. Assume each R_i is convex, so that $\vec{r}_i \in R_i$ (where the symbol $\in$ means "is an element of the set of points"). Define the matrix

$$u_{ij} = \begin{cases} 1 & \text{if } \vec{r}_i \in S_j \cap R_i \\ 0 & \text{if not} \end{cases} \tag{7}$$

Under certain geometric conditions, discussed below, it is reasonable to approximate $w_{ij}\, f_i$ by $u_{ij}\, f_i$, so that

$$p_j \approx \sum_{i=1}^{n} u_{ij}\, f_i \qquad j=1,\ldots,m \tag{8}$$

For each passage S_j we have succeeded in approximating the integral of $f(\vec{r})$ in Equation 1

$$\int_{S_j} f(\vec{r})\, d\vec{r} \tag{9}$$

by the sum of the estimates f_i at a finite set of points within S_j. For a given passage S_j the number of points it intersects

$$N_j = \sum_{i=1}^{n} u_{ij} \qquad j=1,\ldots,m \tag{10}$$

must be nonzero. This limits the coarseness of the division of R.

The shape of the passages S_j does not enter into the formulation of the reconstruction problem in terms of Equations 1. However, in the case of projections obtained from radiation transmitted through the region R, we may call each passage S_j a <u>ray</u> since it goes more or less in a straight line. If R is a convex region of d-dimensional space (divided into n elements R_i all of the same size), then the mean distance across R will be approximately $n^{1/d}$ (where the unit of length is the linear dimension of each R_i). The centroids $\vec{r}_i$ within S_j should be distributed along its length in order to accurately represent the density distribution along S_j. For those rays S_j which roughly coincide with a diameter of R, we will then require $N_j > n^{1/d}$, which sets a more stringent requirement on the coarseness of the division of R.

The centroids contained in the passage S_j are supposed to represent the integral of $f(\vec{r})$ within S_j:

$$p_j \approx \int_{S_j} f(\vec{r})\, d\vec{r} = \sum_{i=1}^{n} \int_{S_j \cap R_i} f(\vec{r})\, d\vec{r} \approx \sum_{i=1}^{n} w_{ij} f_i \qquad j=1,\ldots,m \tag{11}$$

However, the use of the matrix $\{u_{ij}\}$ means that the centroids actually represent

$$\sum_{i=1}^{n} u_{ij} f_i = \sum_{i \ni \vec{r}_i \in S_j} \int_{R_i} f(\vec{r})\, d\vec{r} \qquad j=1,\ldots m \tag{12}$$

(The symbol $\ni$ means "such that".) In general the sum of integrals in Equation 12 will differ from the sum in Equation 11. We may formulate an approximate geometric correction c_j for this discrepancy

$$\sum_{i=1}^{n} \int_{S_j \cap R_i} f(\vec{r})\, d\vec{r} \approx c_j \sum_{i \ni \vec{r}_i \in S_j} \int_{R_i} f(\vec{r})\, d\vec{r} \qquad j=1,\ldots,m \tag{13}$$

where

$$c_j = \frac{\sum_{i=1}^{n} \int_{S_j \cap R_i} d\vec{r}}{\sum_{i \ni \vec{r}_i \in S_j} \int_{R_i} d\vec{r}} \qquad j=1,\ldots,m \tag{14}$$

which simplifies to

$$c_j = \frac{\int_{S_j} d\vec{r}}{N_j \int_{R_1} d\vec{r}} \qquad j=1,\ldots,m \tag{15}$$

provided that all elements R_i have the same size. From Equations 11, 12 and 13 it follows that:

$$p_j \approx c_j \sum_{i=1}^{n} u_{ij} f_i \qquad j=1,\ldots,m \tag{16}$$

This is equivalent to the geometric approximation that

$$w_{ij} \approx c_j u_{ij} \qquad i=1,\ldots,m;\ j=1,\ldots m \tag{17}$$

which can only be true on the average.

It is sometimes possible to choose the projection and reconstruction elements in such a way that c_j is a constant independent of j. For example, consider the reconstruction space $\mathcal{R}$ to be a two-dimensional square divided into n equal squares $\mathcal{R}_i$, i=1,...n, arranged on a grid. A projection of parallel rays at angle θ (for which the $\mathcal{S}_j$ are strips across $\mathcal{R}$), project onto a one-dimensional line (Figure 1). Choose a ray width

$$r_\theta = \min(\,|\sin\theta|,\ |\cos\theta|\,) \tag{18}$$

In this case the strip $\mathcal{S}_j$ intersects one centroid $\vec{r}_i$ per row of elements of $\mathcal{R}$ (except for edge effects). The area of $\mathcal{S}_j$ per row of elements of $\mathcal{R}$ is equal to the area of one element $\mathcal{R}_i$. Thus in Equation 15 we find $c_j \equiv 1$. This justifies the use of Equation 8.

When the geometry requires that c_j not be a constant, we may nevertheless preprocess the data so that

$$p'_j = \frac{p_j}{c_j} \approx \sum_{i=1}^{n} u_{ij} f_i \qquad j=1,\ldots,m \tag{19}$$

Thus it is not necessary to use the weights w_{ij} with, for example, divergent rays, for which c_j depends on j.

We may rewrite Equation 19 as

$$\frac{p_j}{c_j} = \sum_{i\ni\vec{r}_i\in\mathcal{S}_j} f_i \qquad j=1,\ldots,m \tag{20}$$

IV. The Original ART Algorithm

Gordon, Bender & Herman (1970) formulated the ART algorithm in terms of Equation 20, under the implicit assumption that $c_j \equiv 1$. (The justification, using Equation 18, was found later.) Since the algorithm is iterative, let f_i^q designate the q^{th} estimate for f_i. Let

$$p_j^q = c_j \sum_{i\ni\vec{r}_i\in\mathcal{S}_j} f_i^q \qquad j=1,\ldots,m \tag{21}$$

be the value of the projection of the q^{th} estimate. Let $\bar{f}$ be the mean density of the object in $\mathcal{R}$. Then the ART algorithm is

$$f_i^0 \equiv \bar{f} \qquad i=1,\ldots,n \tag{22}$$

$$f_i^{q+1} = \max\left[0,\ f_i^q + \left(\frac{p_j}{c_j} - \frac{p_j^q}{c_j}\right)/N_j\right] \qquad i\ni\vec{r}_i\in\mathcal{S}_j;\ j=1+\mathrm{mod}_m q;\ q=0,\ldots,Km-1 \tag{23}$$

We may express this in words as follows. The iterative process is started with all reconstruction elements set to a constant ($f_i^0=\bar{f}$). In each iteration the difference between the actual data for a projection element and the sum of the reconstruction elements representing it (Equation 21) is calculated $\left(\frac{p_j}{c_j} - \frac{p_j^q}{c_j}\right)$. The correction is evenly divided amongst the (N_j) reconstruction elements ($i\ni\vec{r}_i\in\mathcal{S}_j$) and added to them. If the correction is negative, it may happen that the calculated density for a reconstruction element becomes negative, in which case it is set to zero (max operator, guaranteeing $f_i^q \geq 0$). Each projection element is considered in turn

$(j=1+\mathrm{mod}_m q)$. The calculation is repeated a number of cycles (K) for the whole set of projection elements until reasonable convergence it attained.

The mean density of the object is

$$\bar{f} = \frac{\int_{\mathcal{R}} f(\vec{r})\, d\vec{r}}{\int_{\mathcal{R}} d\vec{r}} \tag{24}$$

$\bar{f}$ may be estimated from a single projection P_k (such as a single x-ray photograph) provided the S_j in projection P_k partition the reconstruction space $\mathcal{R}$:

$$\mathcal{R} = \bigcap_{j \ni S_j \in P_k} S_j \quad \text{and} \quad S_j \cap S_{j'} = \begin{cases} S_j & \text{if } j=j' \\ \emptyset & \text{if not} \end{cases} \quad \text{for all } j,j' \ni S_j, S_{j'} \in P_k \tag{25}$$

($\{S_j \in P_k\}$ partitions $\mathcal{R}$ if every point $\vec{r} \in \mathcal{R}$ is in exactly one of the S_j.) Then

$$\bar{f} = \frac{\sum_{j \ni S_j \in P_k} \int_{S_j} f(\vec{r})\, d\vec{r}}{\int_{\mathcal{R}} d\vec{r}} \approx \frac{\sum_{j \ni S_j \in P_k} P_j}{\int_{\mathcal{R}} d\vec{r}} \equiv \bar{f}_k \tag{26}$$

The approximation may be improved by averaging over the estimates from each P_k:

$$\bar{f} = \frac{1}{K} \sum_{k=1}^{K} \bar{f}_k \tag{27}$$

where K is the number of projections.

The starting values f_i^0 are often chosen to be identically zero, instead of $\bar{f}$. If we order the projection elements P_j such that all of those from one projection come before those of the next, then f_i^q will be the same in either case after the index j has gone through the first projection P_1.

Alternatively, one may use a rough algorithm such as the summation method (reviewed in Gordon & Herman, 1974) to produce starting values:

$$f_i^0 = \left[\sum_{j \ni S_j \cap \mathcal{R}_i \neq \emptyset} p_j / N_j \right] - (K-1)\bar{f} \tag{28}$$

If each projection P_k, $k=1,\ldots,K$ forms a partition of $\mathcal{R}$, then there are exactly K terms in each summation. The advantage of such an initial estimate is that the sequence in q, $\{f_i^q\}$, should converge more rapidly when $\{f_i^0\}$ is near the final result. However, with underdetermined Equations 20, any distortions introduced by such an initial estimate may be retained. (The summation or "back projection" method often produces "ghosts". See Crowther, DeRosier & Klug, 1970, and Bellman, Bender, Gordon & Rowe, 1971.)

V. Convergence Criteria

It is necessary to determine when an iterative algorithm has converged to a solution which is optimal according to some criterion. Various criteria for convergence have been devised.

Gordon, Bender & Herman (1970) proposed three measures for the convergence of the f_i^q: the discrepancy between the measured and calculated projection elements

$$D^q = \sqrt{\frac{1}{m}\sum_{j=1}^{m}\left(\frac{p_j}{c_j} - \frac{p_j^q}{c_j}\right)^2 / N_j} \tag{29}$$

the nonuniformity or variance

$$V^q = \sum_{i=1}^{n} (f_i^q - \bar{f})^2 \tag{30}$$

and the entropy

$$S^q = \frac{-1}{\ln n}\sum_{i=1}^{n}\left(\frac{f_i^q}{\bar{f}}\right)\ln\left(\frac{f_i^q}{\bar{f}}\right) \tag{31}$$

D^q tends to zero, V^q to a minimum and S^q to a minimum with increasing q.

A test pattern is a known function $f^t(\vec{r})$ which is digitized over the reconstruction elements R_i as $\{f_i^t\}$. The Euclidean distance between the test pattern and its q^{th} estimate is

$$\delta^q = \sqrt{\frac{1}{n}\sum_{i=1}^{n}(f_i^q - f_i^t)^2} \tag{32}$$

Gilbert (1972a) showed that by the criterion $\delta^q/\sqrt{V^q}$ ART begins to converge with increasing q but then diverges provided Equations 8 are inconsistent. The absolute values Gilbert obtained for this criterion were greater than necessary, because he did not use the variable ray widths of Equation 18, which I formulated and were later spelled out in Herman & Rowland (1971). The divergence of ART with inconsistent data is nevertheless real. Therefore, the computation should be stopped before divergence begins. Herman, Lent & Rowland (1973) empirically found that the minimum value of $\delta^q/\sqrt{V^q}$ coincided within one iteration with the stopping criterion

$$|V^{q+1} - V^q| < V^q/100 \tag{33}$$

These difficulties with inconsistent data have led to some of the variations of the ART algorithm.

VI. Variations on ART

A. Generalized ART

We may speak of a generalized ART algorithm A as any iterative function which finds new values for the reconstruction elements intersecting a passage from their old values:

$$f_i^{q+1} = A(f_i^q, \{f_i^q, \ni R_i \cap S_j \neq \emptyset\}, p_j) \qquad i \ni R_i \cap S_j \neq \emptyset \tag{34}$$

The sum of the new reconstruction elements should be closer to the value of the projection element:

$$|p_j^{q+1} - p_j| \leq |p_j^q - p_j| \qquad j = 1 + \mathrm{mod}_m q;\ q = 0, \ldots, Km-1 \tag{35}$$

In general, A will have an explicit dependence on the f_i^q under consideration as indicated in Equation 34.

For example, Gordon, Bender & Herman (1970) suggest a series

$$f_i^{q+1} = \max\left[0, \sum_{l=0}^{\infty} A_l (f_i^q)^l\right] \tag{36}$$

where the coefficients A_l are constrained by the relation

$$p_j^{q+1} \leq A_0 N_j + A_1 p_j^q + \sum_{l=2}^{\infty} A_l \sum_{\ni \vec{r}_i \in S_j} (f_i^q)^l = p_j \tag{37}$$

Only one of the A_ℓ is determined by Equation 37. ART with $c_j \equiv 1$ is the special case

$$\begin{aligned} A_0 &= (p_j - p_j^q)/N_j \\ A_1 &= 1 \\ A_\ell &= 0 \qquad \text{for } \ell \geq 2 \end{aligned} \tag{38}$$

B. Multiplicative ART

Multiplicative ART (Gordon, Bender & Herman, 1970) is specified by

$$f_i^{q+1} = \left(\frac{p_j}{p_j^q}\right) f_i^q \tag{39}$$

which corresponds to

$$\begin{aligned} A_0 &= 0 \\ A_1 &= p_j/p_j^q \\ A_\ell &= 0 \qquad \text{for } \ell \geq 2 \end{aligned} \tag{40}$$

in Equation 36. (The same algorithm was found independently by Schmidlin, 1972.)

The choice between additive ART (Equation 23) and multiplicative ART depends on the physics of the radiation used. For transmitted radiation, the form of the reconstructed object should be independent of an additive constant. Such a constant may result from variable exposure in an x-ray, variable development of the film, or an intervening filter, such as the amorphous material increasingly deposited on a sample by the electron beam in electron microscopy. Except for the nonlinearity of the max operator, independence from an additive constant is accomplished by Equation 23, additive ART. However, in nuclear medicine emitted radiation is measured. The count may change rapidly with short-lived radioactive elements but the proportions from one region to another determine the form. In this case a multiplicative algorithm, such as Equation 39, will preserve the form independent of time variation between projections. (It may, of course, be possible to simply normalize the projections in some cases before reconstruction.)

Multiplicative ART must be started with some $f_i^0 > 0$. It has an advantage over additive ART that once $f_i^q \equiv 0$, then it remains so in all subsequent iterations. Clearly all $f_i \ni R_i \cap S_j \neq \emptyset$ should, in general, be set to zero and remain so when $p_j \equiv 0$ (cf. Budinger & Gullberg, 1974). These reconstruction elements demark the subregion of R containing the object being reconstructed.

C. Unconstrained ART

In order to have a version of ART which can be analyzed by the methods of linear algebra, Herman, Lent & Rowland (1973) introduced unconstrained ART for which

$$f_i^{q+1} = f_i^q + w_{ij}(p_j - p_j^q)/N_j \tag{41}$$

where N_j is redefined by

$$N_j = \sum_{i=1}^{n} w_{ij}^2 \qquad j=1,\ldots,m \tag{42}$$

When the matrix $\{w_{ij}\}$ is replaced by $\{u_{ij}\}$ using Equation 17, Equation 42 becomes equivalent to Equation 10. Equation 41 is the same as the iterative matrix inversion method of Kaczmarz (1937).

Unconstrained ART has been proven to converge to the unique solution $\{f_i\}$ minimizing the variance

$$V = \sum_{i=1}^{n} (f_i - \bar{f})^2 \tag{43}$$

when Equations 6 are consistent. On data inconsistent with Equations 6 unconstrained ART converges cyclically, i.e., the f_i^q will be the same after each cycle, for large K.

The algorithm used in the EMI-Scanner (Hounsfield, 1972) is equivalent to unconstrained ART though the geometric correction factor c_j is calculated in a manner different from Equation 15.

Unconstrained ART, of course, permits solutions with some $f_i < 0$, i.e., negative densities.

D. Constrained ART

Fully constrained ART is defined by

$$f_i^{q+1} = \min\left[F, \max[0, f_i^q + w_{ij}(p_j - p_j^q)/N_j] \right] \tag{44}$$

resulting in $0 \le f_i^q \le F$. This constraint may be useful when the object being reconstructed is known to have densities less than F. Herman, Lent & Rowland (1973) chose F = 1 which precludes solutions in integers.

Partially constrained ART (another name for ART, Equation 23) and fully constrained ART have been proven to converge to a solution of Equations 6 when the equations are consistent. However, the solution is not necessarily the one of minimum variance (Equation 43). On inconsistent data, partially and fully constrained ART are conjectured to converge cyclically (Herman, Lent & Rowland, 1973).

E. ART2

ART2 (Herman, Lent & Rowland, 1973) uses an intermediate estimator $\tilde{f}_i^q$

$$\tilde{f}_i^{q+1} = \tilde{f}_i^q + w_{ij}(p_j - p_j^q)/N_j \tag{45}$$

with

$$f_i^{q+1} = \max(0, \tilde{f}_i^{q+1}) \tag{46}$$

in the partially constrained version or

$$f_i^{q+1} = \min[F, \max(0, \tilde{f}_i^{q+1})] \tag{47}$$

in fully constrained ART2. p_j^q is still defined in terms of the f_i^q, not $\tilde{f}_i^q$:

$$p_j^q = \sum_{i=1}^{n} w_{ij} f_i^q \qquad j=1,\ldots m \tag{48}$$

The intermediate estimator may become negative at one iteration and return to zero or a positive value at a later iteration. This is an improvement over ART for which a positive correction always leads to a positive f_i^q.

ART2 and fully constrained ART2 have been shown to converge to the solution of minimum variance (Equation 43) when Equations 6 are consistent.

E. ART3

ART3 (Herman, 1974) was designed to find a solution of Equations 6 within a preset error tolerance which may vary from one projection element to another:

$$p_j - \epsilon_j \le \sum_{i=1}^{n} w_{ij} f_i \le p_j + \epsilon_j \qquad j=1,\ldots,m \tag{49}$$

The algorithm is (Johnson et al., 1973)

$$f_i^{q+1} = f_i^q + \gamma_j^q w_{ij}/N_j \tag{50}$$

where

$$\gamma_j^q = \begin{cases} p_j - p_j^q & \text{if } |p_j - p_j^q| > 2\epsilon_j \quad (51a) \\ 2(p_j - p_j^q - \epsilon_j) & \text{if } \epsilon_j < p_j - p_j^q \le 2\epsilon_j \quad (51b) \\ 2(p_j - p_j^q + \epsilon_j) & \text{if } \epsilon_j > p_j - p_j^q \ge -2\epsilon_j \quad (51c) \\ 0 & \text{if } |p_j - p_j^q| \le \epsilon_j \quad (51d) \end{cases}$$

Equation 6 may be thought of as defining a hyperplane in n-dimensional space and Inquality 49 a 'hyperslab'. Condition 51a results in a projection of the n-dimensional point $\{f_i^q\}$ onto the hyperplane of Equation 6 and is equivalent to unconstrained ART (Equation 41). A point within a distance ϵ_j of the hyperslab is reflected about the nearest face of the hyperslab by Conditions 51b or 51c. If point $\{f_i^q\}$ is already within the hyperslab, no correction is made (Condition 51d).

ART3 may be shown to converge to a solution of Inequality 49 in a finite number of iterations, provided a solution exists.

G. ART with Binary Constraint

An ART method for binary patterns (f_i = 0 or 1, i=1,...,n) based on ART2 and ART3 has been presented by Herman (1973).

Gilbert (1972b) has given a method, applicable to any iterative algorithm, which yields a two-valued $\{f_i\}$. The densities are divided into two groups after a few iterations, and each f_i is set to the mean of its group. The procedure is repeated in subsequent iterations.

This manner of introducing a nonlinear constraint into a reconstruction may be of widespread usefulness. As an example, the known densities of tissues might be incorporated in x-ray reconstructions (H. Blum, personal communication).

H. ART with a Damping Factor

The introduction of a damping factor Δ as in

$$f_i^{q+1} = f_i^q + \Delta\, w_{ij}(p_j - p_j^q)/N_j \tag{52}$$

leads only to a partial correction if $0 < \Delta < 1$. Sweeney & Vest (1973) found that $\Delta \leq 0.5$ improved the reconstruction. If the projection elements s_j are considered in random order within a cycle, both rapid convergence and tolerance to noise (inconsistent equations) are obtained (S. A. Johnson, personal communication).

I. Minimizing Local Discontinuity

Kashyap & Mittal (1973) have introduced the notion that a desirable solution to Equations 6 is one minimizing the variance (Equation 43) plus a measure of the local discontinuity

$$J(\alpha) = V + \alpha \sum_{i=1}^{n} (f_i - \frac{1}{8} \sum_{i'} f_{i'})^2 \tag{53}$$

where the space $\mathcal{R}$ is two-dimensional and i' ranges over the eight elements $\mathcal{R}_{i'}$ closest to $\mathcal{R}_i$ (on a square lattice). Such a function explicitly takes into account the fact that the $\{f_i\}$ represents an object whose density should vary in a piecewise continuous fashion. Equation 53 may be generalized for any d-dimensional reconstruction space $\mathcal{R}$:

$$J(\alpha) = V + \alpha \sum^{n} (f_i - \sum_{i'=1}^{n} \eta_{ii'} f_{i'})^2 \tag{54}$$

where $\{\eta_{ii'}\}$ is a matrix describing the weights to be attributed to each of the near neighbors of the reconstruction element $\mathcal{R}_i$. ($\{\eta_{ii'}\}$ is a sparse matrix: each row contains at most $3^d - 1$ nonzero elements if the $\mathcal{R}_i$ are arranged in a d-dimensional cubic lattice.)

Although Kashyap & Mittal (1973) invert the resulting matrix directly (which requires an enormous amount of computing time), Equation 53 may be incorporated into ART-type algorithms for rapid iterative solution.

The second part of $J(\alpha)$ would be minimized if

$$f_i - \sum_{i'=1}^{n} \eta_{ii'} f_{i'} = 0 \qquad i=1,\ldots,n \tag{55}$$

which may simply be regarded as n homogeneous equations of the form of Equations 6. These may be solved simul-

taneously with Equations 6 by any of the ART algorithms tolerant to inconsistent data. (Equations 55 have the unique solution $f_i \equiv 0$ if the matrix $\{\delta_{ii'} - \eta_{ii'}\}$ is nonsingular, which depends on the boundary conditions.) Equations 6 and 55 together form a system of $n + m$ overdetermined equations. Each Equation 55 geometrically represents a "passage" confined to a local group of reconstruction elements.

A continuum approach leads to another formulation of an ART-like algorithm. The limit of Equation 54 as the subdivision of $\mathcal{R}$ gets finer:

$$J(\alpha) = \int_{\mathcal{R}} [f(\vec{r})-\bar{f}]^2 \, d\vec{r} + \alpha \int_{\mathcal{R}} [\nabla^2 f(\vec{r})]^2 \, d\vec{r} \qquad (56)$$

transforms the reconstruction problem into a problem in the calculus of variations (Gordon & Kashyap, 1974). This opens the reconstruction problem to solution by numerical methods for partial differential equations.

For example, the matrix $\{\eta_{ii'}\}$ is equivalent to the finite difference schemes used to solve partial differential equations. If the general ART algorithm of Equation 34 is restricted to

$$f_i^{q+1} = f_i^q + A(\{f_{i'}^q\}, p_j) \qquad i \ni \mathcal{R}_i \cap \mathcal{S}_j \neq \emptyset \qquad (57)$$

we can see that it represents the Eulerian numerical approximation to the partial differential equation

$$\frac{\partial f(\vec{r},q)}{\partial q} = A(f(\vec{r},q), \{p_j\}) \qquad (58)$$

Appropriate forms for A are given by Gordon & Kashyap (1974).

J. Monte Carlo Algorithm

The first Monte Carlo algorithm of Gordon & Herman (1971a,b) solved Equations 20 in integers. For each projection element p_j corrections were made by adding or subtracting 1 at random to the $f_i \ni \mathcal{R}_i \cap \mathcal{S}_j \neq \emptyset$ with the constraint that $f_i \geq 0$. The statistical mean of this process is equivalent to ART. Smooth reconstructions were obtained by averaging a number of Monte Carlo solutions. The limit of such averaging yields the same reconstruction as ART. (Frank, 1973, mislabels ART as a Monte Carlo method.)

VII. The Reliability of ART Reconstructions

Resolution criteria and the performance of reconstruction algorithms according to these criteria have been reviewed by Gordon & Herman (1974). In general, these criteria produce a single number, such as the δ of Equation 32, whose relationship to the visual quality of the reconstruction is only heuristic. Thus, I will only discuss two methods for obtaining visual measures for the reliability of reconstruction algorithms.

Equations 6 are ordinarily highly underdetermined, so that there exists an infinity of solutions. Any deterministic algorithm locates only one of these solutions. Unless the noise in the data is extreme, the original object is also amongst the solutions. If we had before us sample solutions from the whole space of solutions, these might have some features in common with one another. Other features might be shared only by certain subsets of the solutions. The former will be called real features, since they must be part of the original object. The latter features are suspect, since they may or may not be included in the original object (Gordon, 1973).

It is only necessary to demonstrate two solutions, one with and one without a given feature, to label that feature as suspect. However, without seeing samples from the whole space of solutions, we can at best form a heuristic guide to the real features.

Given any iterative algorithm, we may start it off with an arbitrary function $\{f_i^0\}$ and then iterate to convergence. Each different $\{f_i^0\}$ may generate a different solution to Equations 6. If we had a systematic way of generating the $\{f_i^0\}$, then we could explore the space of solutions.

Gordon (1973) proposed starting this exploration with the "ordinary" initial value $f_i^0 = \text{constant}$, say $= 0$ for an additive algorithm. Let $\{f_i(0)\}$ designate the reconstruction so obtained. This reconstruction will

contain various features visible to the eye. These features may be removed by setting the corresponding $f_i(0)$ within the feature to another value, say 0 or the surrounding density. The resulting function, $\{f_i'\}$, may now be used as the starting function, to obtain a new reconstruction $\{f_i(\{f_i'\})\}$. If the feature is not contained in the new reconstruction, then it is suspect. If it does appear, we gain some confidence in its reality, since its reappearance was apparently forced by the data. This notion is strengthened by the empirical observation that manipulations of this type made on a local region of a reconstruction have only minor consequences for other regions. (This phenomenon occurs in spite of the fact that the passages S_j cross the reconstruction space R, so that regions far apart are mingled in the data $\{p_j\}$.)

Many reconstructions can accumulate from the various features seen in $\{f_i(0)\}$. Three operators are given for combining the solutions in a way which attempts to visually preserve their common features (Gordon, 1973).

Barbieri (1974) makes deliberate use of the nonlinear constraint $f_i \geq 0$ to produce a function which may visualize the regions in which the reconstruction is unreliable. Let

$$F = \max_{i=1,\ldots,n} f_i \tag{59}$$

Then the complement of $\{f_i\}$ is defined as

$$\hat{f}_i = F - f_i \qquad i=1,\ldots,n \tag{60}$$

Thus Equations 6 may be rewritten as

$$p_j \approx \sum_{i=1}^{n} w_{ij} f_i = F\sum_{i=1}^{n} w_{ij} - \sum_{i=1}^{n} w_{ij} \hat{f} = \left(F\sum_{i=1}^{n} w_{ij}\right) - \hat{p}_j \qquad j=1,\ldots m \tag{61}$$

which defines the complementary projection data $\{\hat{p}_j\}$. Let $\{f_i\}$ and $\{\hat{f}_i\}$ be solutions by some algorithm of Equations 6 and the complementary equations

$$\hat{p}_j \approx \sum_{i=1}^{n} w_{ij} \hat{f}_i \qquad j=1,\ldots,m \tag{62}$$

Define

$$\omega_i = f_i + \hat{f}_i \qquad i=1,\ldots,n \tag{63}$$

If the algorithm were linear, we would expect $\omega_i \equiv F$, $i=1,\ldots,n$. If it is not linear, $\{\omega_i\}$ will depart from the constant F. Barbieri (1974) suggests that those subregions of R in which the ω_i depart significantly from F are less reliably reconstructed than the others. This conjecture warrants further testing and theoretical justification.

Barbieri (1974) further suggests a modification of ART-type algorithms. After calculating both f_i^q and $\hat{f}_i^q$ in the ordinary manner, one adds to each

$$\frac{1}{2}\left(F - \omega_i^q\right) \tag{64}$$

where

$$\omega_i^q = f_i^q + \hat{f}_i^q \tag{65}$$

In some sense this procedure provides a step by step balance and seems to yield a cleaner reconstruction.

Other visual criteria for the reliability of reconstructions will come from future psychophysical experiments on the probability of detecting features and double-blind experiments on the accuracy of medical diagnoses based on reconstructions.

VIII. Efficiency in Computing

Because of the size of the reconstruction problem, it is necessary to pay strict attention to computing efficiency. I will propose some general guidelines.

Equations 19 allow a substantial increase in computing speed over Equations 6. Since the u_{ij} are all 0's or

1's, it is not necessary to perform the multiplication $u_{ij} f_i$. One need only determine which reconstruction elements have centroids lying in S_j, as in Equation 20. Moreover, the data can be scaled so that p_j/c_j is an integer. We then seek a solution to Equations 20 for which the f_i are all integers. (Equations 20 are then Diophantine equations.)

A single term in the summation in Equations 19 or 20 then requires only an integer addition in a computer, whereas a term of Equations 6 requires both a floating point multiplication and a floating point addition. Moreover, there are many more nonzero w_{ij} than nonzero u_{ij}. Floating point multiplication or addition takes 5 to 7 times longer on computers than integer addition. Thus algorithms based on Equations 19 or 20 can be more than 10 times faster than those based on Equations 6.

A number of other devices may be used to reduce the size of the reconstruction problem or increase its computational speed. For instance, the number of projections can be minimized consistent with the desired 'resolution' in the reconstruction space. (See Gordon, Bender & Herman, 1970, for sequences of reconstructions with increasing numbers of projections, and Gordon & Herman, 1974, for a review of resolution criteria.)

The skillful use of machine language will also reduce computing time. The innermost loop of an iterative algorithm, such as ART, may be written in machine language and repeated in consecutive memory locations. This stack of instructions is then entered at the appropriate point so that the number remaining is exactly the number needed for a given projection element. A stack makes it unnecessary to increment an index, which can save 40% computing time for the ART algorithm.

Finally, special purpose computers may be considered. For instance, the Array Transform Processor by Raytheon can speed an iterative algorithm a hundredfold over a comparable general purpose computer. Optical or electronic analog or hybrid devices might achieve even greater speeds. This is emphasized by the fact that the multi-view tomograph device of Grant (1972) can achieve a full three dimensional x-ray reconstruction by optical means in a time comparable to that required by the EMI-Scanner to reconstruct a few planes.

It is important to compare the capabilities of the EMI-Scanner with the multi-view tomograph. The EMI-Scanner achieves accurate values for the densities f_i, but is restricted to 50 x 50 reconstruction elements across the head. (3 mm x 3 mm for each R_i. The latest model allows 1.5 mm x 1.5 mm.) The 20-view tomograph has a modulation transfer function (MTF) which falls off to 10% between 1.3 and 6.2 cycles/mm (Meyer, 1969, Figure 13). This roughly corresponds to an optical resolution of 0.15 to 0.5 mm (Biberman, 1973, Table 2.1). If we were to consider reconstruction elements of these dimensions, we would need 700 x 700 x 700 to 3700 x 3700 x 3700 for the equivalent spatial resolution or 3×10^7 to 5×10^{10} elements. Because the tomographic reconstruction algorithm is rough (Gordon & Herman, 1974), the individual f_i are inaccurate. There is in general a trade-off between spatial and density resolution; however, the optimum balance has not yet been achieved.

IX. Conclusion

There are four major classes of reconstruction algorithms: the summation methods (of which classical tomography is a prime example), the convolution method, the Fourier methods and series expansion methods (Gordon & Herman, 1974). ART algorithms belong to the latter category.

All ART algorithms use the same basis set, the division of the reconstruction space into nonoverlapping elements. All share the property of iteratively attempting to match the (weighted or unweighted) sums of appropriate reconstruction elements with the corresponding projection data.

We can expect numerous versions of the ART algorithms to be developed in the future because of their intuitive simplicity and wide margin for variation. Future ART algorithms will undoubtedly include versions for use on parallel computers and analog hardware implementations. We may also look forward to a more thorough mathematical analysis of linear ART algorithms and those which are linear with simple inequality constraints.

Acknowledgements

I would like to thank Leslie Gordon, J. Z. Hearon, Helmut V. B. Hirsch and Rosalind Marimont for critical reading of the manuscript and Marian Caesar for careful typesetting.

Table 1. Symbols

A	generalized ART-like recursive function (Equation 34)
A_ℓ	ℓ^{th} term of generalized ART-like algorithm which can be represented by a series expansion (Equation 36)
ART	Algebraic Reconstruction Technique(s)
α	weight for the local discontinuity in $J(\alpha)$ (Equation 53)
c_j	geometric correction for the representation of the integral over a passage g_j by the sum of the values at the centroids $\vec{r}_i$ contained in the passage (Equations 13, 14)
d	dimension of the reconstruction space R
$d\vec{r}$	an area or volume element of the reconstruction space R (if d=2, $d\vec{r}$ = dxdy; if d = 3, $d\vec{r}$ = dxdydz; etc., Equation 1)
D^q	mean discrepancy between measured projection elements p_j and their estimate at the q^{th} iteration, p_j^q (Equation 29)
δ^q	Euclidean distance between a test pattern $\{f_i^t\}$ and its reconstruction at the q^{th} iteration (Equation 32)
$\delta_{ii'}$	= 1 if i = i', = 0 if not
Δ	damping factor (Equation 52)
ϵ	"is an element of"
ϵ_j	error margin for the j^{th} projection element (Equation 49)
$\ni$	"such that"
f	unknown density function (Equation 1)
$\bar{f}$	mean of the unknown density function f over the reconstruction space R (Equation 26)
f_i	estimate for the density function f in the reconstruction element R_i (Equation 3)
f_i^q	q^{th} estimate for f_i (Equation 21)
$\tilde{f}_i^q$	intermediate estimator for f_i^q (Equation 45)
$\hat{f}_i$	complement of f_i (Equation 60)
$\hat{f}_i^q$	complement of f_i^q (Equation 65)
f^t	known density function or test pattern (Equation 32)
f_i^t	average of f^t over the reconstruction element R_i (Equation 32)
F	maximum density (Equation 44)
γ_j^q	correction factor for ART3 (Equations 50, 51)
i	subscript for reconstruction elements (Equation 2)
j	subscript for projection elements (Equation 1)
k	subscript for projections (Equation 25)
K	number of cycles of using each projection element once (Equation 23)
κ	number of projections (Equation 27)
ℓ	subscript on series A_ℓ (Equation 36)
m	number of projection elements (Equation 1)
max	max(a,b) = a if a > b, = b if b ≥ a
min	min(a,b) = a if a < b, = b if b ≤ a
mod	$\text{mod}_m q$=remainder when q is divided by m
n	number of reconstruction elements R_i (Equation 2)
N_j	number of centroids $\vec{r}_i$ intersected by g_j (Equation 10) or its generalization (Equation 42)
$\eta_{ii'}$	weight for the contribution of reconstruction element $R_{i'}$ to R_i in $J(\alpha)$ (Equation 54)
$\emptyset$	the empty set
p_j	density measurement of the j^{th} projection element (Equation 1)
p_j'	geometrically corrected density of the j^{th} projection element (Equation 19)
$\hat{p}_j$	complement of p_j (Equation 61)
p_j^q	density of the j^{th} projection of $\{f_i^q\}$ (Equation 21)
P_k	the set of passages g_j corresponding to the k^{th} projection (Equation 25)
ρ_j	projection element
q	iteration counter, incremented each time an iterative algorithm goes from one projection element to the next (Equation 21)
$\vec{r}$	a point in the reconstruction space R (Equation 1)
$\vec{r}_i$	centroid of reconstruction element R_i (Equation 7)
r_θ	width of a parallel ray at angle θ (Equation 18)
R	reconstruction space (the domain of f)
R_i	i^{th} reconstruction element (Equation 2)
S^q	entropy of $\{f_i^q\}$ (Equation 31)
g_j	passage through R traversed by radiation reaching projection element ρ_j (Equation 1)
θ	angle (Equation 18)
u_{ij}	indicates intersection of centroid $\vec{r}_i$ with passage g_j (Equation 7)
V	variance of $\{f_i\}$ (Equation 43)
V^q	variance of $\{f_i^q\}$ (Equation 30)
w_{ij}	fraction of reconstruction element R_i intersected by passage g_j (Equation 4)
ω_i	sum of f_i and $\hat{f}_i$ (Equation 63)

ω_i^q sum of f_i^q and $\hat{f}_i^q$ (Equation 65)

$\{\ \}$ "the set"

$\cap$ "intersection of"

∇^2 Laplacian, $\frac{\partial^2}{\partial x^2} + \frac{\partial^2}{\partial y^2}$ in two dimensions, etc. (Equation 56)

References and Bibliography on ART-like Algorithms

M. Barbieri (1974). A criterion to evaluate three dimensional reconstructions from projections of unknown structures. J. Theor. Biol., in press.

S. H. Bellman, R. Bender, R. Gordon & J. E. Rowe, Jr. (1971). ART is science, being a defense of algebraic reconstruction techniques for three-dimensional electron microscopy. J. Theor. Biol. 32, 205-216.

R. Bender, S. H. Bellman & R. Gordon (1970). ART and the ribosome: a preliminary report on the three-dimensional structure of individual ribosomes determined by an algebraic reconstruction technique. J. Theor. Biol. 29, 483-487.

L. M. Biberman (1973). Perception of Displayed Information. Plenum Press, New York and London.

T. F. Budinger & G. T. Gullberg (1974). Three-dimensional reconstruction in nuclear medicine by iterative least-squares and Fourier techniques. Lawrence Berkeley Laboratory, University of California, LBL-2146, 133 pp.

Correspondent (1971). The ART of the possible. Nature New Biology 232, 131.

R. A. Crowther, D. J. DeRosier & A. Klug (1970). The reconstruction of a three-dimensional structure from projections and its application to electron microscopy. Proc. Roy. Soc. Lond. A 317, 319-340.

R. A. Crowther & A. Klug (1971). ART and science, or, conditions for 3-D reconstruction from electron microscope images. J. Theor. Biol. 32, 199-203.

J. Frank (1973). Computer processing of electron micrographs. In: Electron Microscopical Techniques in Biology, J. Koehler, ed., Springer Verlag, Heidelberg, pp. 215-274.

P. Gilbert (1972a). Iterative methods for the reconstruction of three-dimensional objects from projections. J. Theor. Biol. 36, 105-117.

P.F.C. Gilbert (1972b). An iterative method for three-dimensional reconstruction from electron micrographs. Proc. Fifth European Congr. on Electron Microscopy, pp. 602-603.

R. Gordon (1973). Artifacts in reconstructions made from a few projections. Proceedings of the First International Joint Conference on Pattern Recognition, Oct. 30 to Nov. 1, Washington, D.C., IEEE Computer Society, Publications Office, 9017 Reseda Boulevard, Suite 212, Northridge, California 91324, pp. 275-285.

R. Gordon (1974). A comprehensive bibliography on reconstruction from projections. Methods of Information in Medicine, in press.

R. Gordon & R. Bender (1971). New three-dimensional Algebraic Reconstruction Techniques (ART). Proc. 29th Annual Meeting Electron Microscopy Society of America, Boston, 9-13 August, 82-83.

R. Gordon, R. Bender & G. T. Herman (1970). Algebraic reconstruction techniques (ART) for three-dimensional electron microscopy and x-ray photography. J. Theor. Biol. 29, 471-481.

R. Gordon & G. T. Herman (1971a). Reconstruction of pictures from their projections. Quarterly Bulletin of the Center for Theoretical Biology, State University of New York at Buffalo 4(1), 71-151.

R. Gordon & G. T. Herman (1971b). Reconstruction of pictures from their projections. Comm. A.C.M. 14(12) 759-768. (Figs. 6 and 7 are interchanged.)

R. Gordon & G. T. Herman (1974). Three dimensional reconstruction from projections: A review of algorithms. Int. Rev. Cytol. 38, in press.

R. Gordon & R. L. Kashyap (1974). Variational formulations of the problem of reconstruction from projections, in preparation.

R. Gordon, J. E. Rowe, Jr. & R. Bender (1971). ART: a possible replacement for x-ray crystallography at moderate resolution. First European Biophysics Congress, Baden near Vienna, September 14-17, E XVIII/4, 441-445.

D. G. Grant (1972). Tomosynthesis: A three-dimensional radiographic imaging technique. IEEE Trans. Bio-med. Eng. BME19(1), 20-28.

J. F. Greenleaf, S. A. Johnson, S. L. Lee, G. T. Herman & E. M. Wood (1974). Algebraic reconstruction of spatial distributions of acoustic absorption within tissue from their two-dimensional acoustic projections. Acoustic Holography 5, 591-603.

G. T. Herman (1972). Two direct methods for reconstructing pictures from their projections: a comparative study. Computer Graphics and Image Processing 1(2), 123-144.

G. T. Herman (1974). Reconstruction of binary patterns from a few projections. International Computing Symposium, Davos, Switzerland, 4-7 September 1973, editors A. Guenther, et al., North Holland Publ. Co., pp. 371-379.

G. T. Herman (1974). A relaxation method for reconstructing objects from noisy x-rays, submitted to Mathematical Programming.

G. T. Herman, A. Lent & S. Rowland (1973). ART: Mathematics and applications. A report on the mathematical foundations and on the applicability to real data of the Algebraic Reconstruction Techniques. J. Theor. Biol. 42(1), 1-32.

G. T. Herman & S. Rowland (1971). Resolution in ART: an experimental investigation of the resolving power of an algebraic picture reconstruction technique. J. Theor. Biol. 33, 213-223.

G. T. Herman & S. Rowland (1974). Three methods for reconstructing objects from x-rays: a comparative study. Computer Graphics and Image Processing, in press.

G. N. Hounsfield (1972). A method of and apparatus for examination of a body by radiation such as x or gamma radiation. The Patent Office, London, Patent Specification 1283915.

S. A. Johnson, R. A. Robb, J. F. Greenleaf, E. L. Ritman, G. T. Herman, S. L. Lee & E. H. Wood (1973). Temporal and spatial x ray projective reconstruction of a beating heart, preprint, Mayo Clinic, Rochester, Minnesota.

S. A. Johnson, R. A. Robb, J. F. Greenleaf, E. L. Ritman, S. L. Lee, G. T. Herman, R. E. Sturm & E. H. Wood (1974). The problem of accurate measurement of left ventricular shape and dimensions from multiplane roentgenographic data. Proceedings of the Second Workshop on Contractile Behavior of the Heart, Utrecht, 6-7 September, 1973. European J. Cardiol., pp. 137-155.

S. Kaczmarz (1937). Angenaeherte Aufloesung von Systemen linearer Gleichungen. Bulletin International des Sciences et des Lettres, Classe des Sciences Mathematiques et Naturelles, Serie A: Sciences Mathematiques, 355-357.

R. L. Kashyap & M. C. Mittal (1973). Picture reconstruction from projections. Proceedings of the First International Joint Conference on Pattern Recognition, Oct. 30 to Nov. 1, Washington, D.C., IEEE Computer Society, Publications Office, 9017 Reseda Boulevard, Suite 212, Northridge, California 91324, pp. 286-292.

R. A. Meyer (1969). 3-D radiography - modulation transfer function. Memo MRT-1-127, 4 December to D. G. Grant, Applied Physics Laboratory, Johns Hopkins University, Silver Spring, Maryland, 25 pp.

P. Schmidlin (1972). Iterative separation of sections in tomographic scintigrams. Nucl. Med. (Stuttg.) 11, 1-16.

P. R. Smith, T. M. Peters & R. H. T. Bates (1973). Image reconstruction from finite numbersof projections. J. Phys. A: Math., Nucl. Gen. 6, 361-382.

D. W. Sweeney & C. M. Vest (1973). Reconstruction of three-dimensional refractive index fields from multidirectional interferometric data. Applied Optics 12(11), 2649-2664.

A. Todd-Pokropek (1973). Tomography and the reconstruction of images from their projections. Third International Conference on Data Handling and Image Processing in Scintigraphy, Massachusetts Institute of Technology, 6-9 June, 1973, in press.

B. K. Vainshtein (1973). (Three-dimensional electron microscopy of biological macromolecules.) Uspekhi Fizicheskikh Nauk 109(3), 455-497.